

BJR



■ BIOMATERIALS

The biological response to laser-aided direct metal-coated Titanium alloy (Ti6Al4V)

**T. Shin,
D. Lim,
Y. S. Kim,
S. C. Kim,
W. L. Jo,
Y. W. Lim**

Seoul St. Mary's
Hospital, The Catholic
University of Korea,
Seoul, South Korea

Objectives

Laser-engineered net shaping (LENS) of coated surfaces can overcome the limitations of conventional coating technologies. We compared the *in vitro* biological response with a titanium plasma spray (TPS)-coated titanium alloy (Ti6Al4V) surface with that of a Ti6Al4V surface coated with titanium using direct metal fabrication (DMF) with 3D printing technologies.

Methods

The *in vitro* ability of human osteoblasts to adhere to TPS-coated Ti6Al4V was compared with DMF-coating. Scanning electron microscopy (SEM) was used to assess the structure and morphology of the surfaces. Biological and morphological responses to human osteoblast cell lines were then examined by measuring cell proliferation, alkaline phosphatase activity, actin filaments, and RUNX2 gene expression.

Results

Morphological assessment of the cells after six hours of incubation using SEM showed that the TPS- and DMF-coated surfaces were largely covered with lamellipodia from the osteoblasts. Cell adhesion appeared similar in both groups. The differences in the rates of cell proliferation and alkaline phosphatase activities were not statistically significant.

Conclusions

The DMF coating applied using metal 3D printing is similar to the TPS coating, which is the most common coating process used for bone ingrowth. The DMF method provided an acceptable surface structure and a viable biological surface. Moreover, this method is automatable and less complex than plasma spraying.

Cite this article: *Bone Joint Res* 2018;7:357–361.

Keywords: Coating technology, Metal 3D printing, Porous coating

■ T. Shin, PhD, Department of Mechanical Engineering, Sejoing University; Corentec, Central R&D Center, Seoul, South Korea.
■ D. Lim, PhD, Associate Professor, Department of Mechanical Engineering, Sejoing University, Seoul, South Korea.
■ Y. S. Kim, MD, PhD, Professor,
■ S. C. Kim, MD, Clinical Instructor,
■ W. L. Jo, MD, PhD, Clinical Assistant Professor,
■ Y. W. Lim, MD, PhD, Assistant Professor, Department of Orthopaedic Surgery, Seoul St. Mary's Hospital, School of Medicine, The Catholic University of Korea, Seoul, South Korea.

Correspondence should be sent to Y-W. Lim; email: albire00@naver.com

doi: 10.1302/2046-3758.75.BJR-2017-0222.R1

Bone Joint Res 2018;7:357–361.

Cementless arthroplasty provides biological fixation with superior durability and enhanced preservation of bone compared with cemented arthroplasty.¹⁻³ Since the stability of a cementless arthroplasty is based on the porous structure formed at the surface of the components, this procedure requires the initial application of a fixation force, excellent adhesion and effective biological fixation.^{1,4,5} Osseointegration can be achieved by offering an optimal porous structure for bone ingrowth by forming pores at the surface of the components similar to that of cancellous bone.^{4,6,7}

The ideal structure contains interconnected macro- (pore size >100 μm) and micro- (pore size < 20 μm) porosity.^{1,4,8} Various surface treatments, including bead coating, fibre metal coating and plasma spraying have been

developed for promoting the ingrowth of bone for cementless components. These methods are widely used with rates of long-term clinical survival that range from 81% to 99% after approximately ten years.⁹⁻¹²

However, Karageorgiou et al¹³ reported that the porosity of conventional surface coatings (30% to 60%) is less than that of cancellous bone (50% to 90%). Additionally, the requirement of heating to over 2000°F during the coating process reduces the fatigue strength of the substrate. Clinical results have been excellent despite these drawbacks. Shin et al¹⁴ introduced laser-engineered net shaping coating technology to overcome the limitations of conventional coatings. They used a 3D additive manufacturing technology, laser-aided direct metal

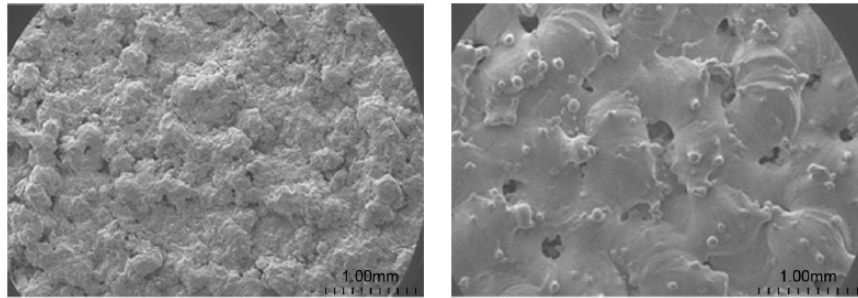


Fig. 1

Scanning electron microscopy images of the surfaces of (a) titanium plasma spray (TPS)-coated (30 \times) and (b) direct metal fabrication (DMF)-coated (30 \times) specimens showing the different surface characteristics. Compared with the TPS-coated surface, the DMF-coating had a more uniform porosity, which ranged from 200 μm to 500 μm .

fabrication (DMF), and evaluated its use as a surface coating technology for artificial joints. A DMF coating has a porosity of about 65% with a pore size ranging from 200 μm to 500 μm , and is about 500 μm thick. It has 17.5% greater tensile strength and 10.2% greater shear strength than a coating applied using titanium plasma spray (TPS). The DMF coating has a better uniform porous structure and has superior mechanical properties to those of coatings provided by other methods.¹⁴ However, the biological responses to a DMF coating have not been reported. We therefore investigated whether *in vitro* responses to TPS-coated and DMF-coated titanium alloy (Ti6Al4V) were biologically different.

Materials and Methods

We compared the cell morphology, confocal microscopy results for RUNX2 gene, the rate of proliferation of cells and the alkaline phosphatase activity of TPS- and DMF-coated Ti6Al4V alloy surfaces *in vitro*. Two groups of Ti6Al4V discs with a diameter of 12 mm and a thickness of 10 mm, were manufactured with 30 being used in each group.

Manufacturing of the specimens. For the TPS technique, an electric arc was generated between two electrodes in a gun. The arc was heated to 20 000 $^{\circ}\text{F}$. The gases were passed through a jet-shaped anode at high speed. The powder for the coating was injected into the plasma gas stream, melted, and impacted onto the substrate at a high kinetic energy to form a porous coating. Varying the operating parameters determined the different degrees of porosity of the coatings.

For the DMF technique, pure titanium (Ti) (grade 2, ASTM F1580) powder was melted and laminated using high-powered laser irradiation to a Ti6Al4V surface. The porous structure was then manufactured using a 3D computer-assisted programme that created a sufficient fixation force by matching the material to the properties of cancellous bone. The surface was irradiated with a laser (power 100 W, scan speed 1.5 m/minute, powder delivery rate 2.2 g/minute) by following a pre-programmed path along a grid, which formed a melted pool. Next, the powders

were sprayed and laminated onto the surface to create a coating whose mean thickness was 500 μm .^{14,15}

The two surfaces were characterized using scanning electron microscopy (SEM) (model JSM-6700F; JEOL Ltd, Tokyo, Japan) after the test specimens had been coated. The SEM results indicated different surface characteristics (Fig. 1). Compared with the TPS surface (Fig. 1a), the DMF surface had a more uniformly porous structure with a mean pore size in the coating of between 200 μm and 500 μm , mean porosity of 65% (SD 5%) and thickness of 500 μm (SD 100 μm)(Fig. 1b).

Culture and osteogenic differentiation of human mesenchymal stem cells. Two passages of human bone marrow-derived mesenchymal stem cells (hMSCs; Catholic Master Cells) were obtained from the Catholic Institute of Cell Therapy (CIC Korea Inc., Seoul, South Korea). The certificates of analysis for the hMSC phenotype confirmed the CD31, CD34 and CD45 negative markers and CD73 and CD90 positive markers. The hMSCs were cultured in Dulbecco's modified Eagle's medium (DMEM) (HyClone; GE Healthcare, Waltham, Massachusetts), 20% foetal bovine serum (FBS) (HyClone; GE Healthcare) with 1% penicillin/streptomycin (Gibco BRL, Grand Island, New York) for five passages. The cells were maintained at 37 $^{\circ}\text{C}$ for 24 hours in a humidified incubator containing 5% CO₂.

Culturing six passages of hMSCs induced osteogenic differentiation according to a StemPro Osteogenesis Differentiation Kit (Thermo Fisher Scientific, Loughborough, UK). The osteogenesis differentiation medium was an osteocyte differentiation basal medium with osteogenesis supplement gentamicin reagent. The hMSCs were seeded in a six-well culture plate at a cell density of 3 \times 10⁴ cells/cm². The media were replaced every three to four days for a total incubation period of 21 days.

Cell morphology. The osteoblasts from the hMSCs were seeded with 5 \times 10⁴ cells on TPS, DMF and machined Ti6Al4V specimens. After six hours of seeding of cells in each implant, the media were removed and the cells were washed three times with phosphate-buffered saline (PBS). These cells were stabilized for two hours after adding 2% glutaraldehyde–PBS solution and then washed

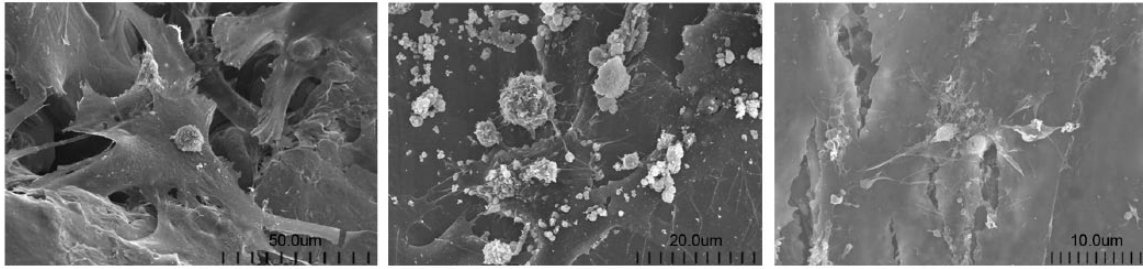


Fig. 2

Scanning electron microscopy (SEM) images show osteoblasts after six hours of incubation on (a) titanium plasma spray (TPS) ($\times 1000$), (b) direct metal fabrication (DMF) ($\times 2000$), and (c) machined Ti6Al4V ($\times 3000$) specimens. In contrast to machined surfaces, DMF and TPS surfaces were largely and strongly covered with healthy lamellipodia of the osteoblasts, and a thin cytoplasmic process branched out from the filopodia to enter a pore.

three times with distilled water. At 30-minute intervals, the cells were dehydrated with 50% to 100% ethanol solutions. The ethanol was removed and the cells were left at room temperature to allow complete evaporation of the ethanol. The two surfaces were then characterized using SEM (model JSM-6700F; JEOL Ltd) after the specimens had been coated with platinum.

Cell proliferation assay. The osteoblasts were seeded with 5×10^4 cells on the TPS, DMF and machined Ti6Al4V specimens, and incubated for 24, 48, 72 and 96 hours. The medium was replaced with fresh medium before measuring cell proliferation using the Cell Titer 96 Non-Radioactive Cell Proliferation Assay (Promega Corp., Madison, Wisconsin), according to the manufacturer's instructions. This assay is a colorimetric method for determining the number of viable cells. In this study, the number of viable cells was measured at 450 nm using an enzyme-linked immunosorbent assay (ELISA) reader (Bio-Tek Instruments Inc., Winooski, Vermont).

Alkaline phosphatase activity. Alkaline phosphatase (ALP) activity was measured by seeding the osteoblasts with 5×10^4 cells in medium containing 1% FBS on TPS, DMF, and machined Ti6Al4V samples, followed by incubation for seven and 14 days. The medium was removed and the cells were washed three times with PBS to remove as much serum in the culture fluid as possible. Next, 1 mL of 0.02% Triton X-100 (Merck KGaA, Darmstadt, Germany) was placed on a sample to lyse the cells. The cytolytic solution was transferred into a 1.5 mL tube, and the cells were sonicated. The tube was centrifuged (14 000 rpm, 4°C, 15 minutes) and the supernatant was transferred to a new 1.5 mL tube. Then, 100 μ L of 1 mol/L Tris-HCl, 20 μ L of 5 mmol/L MgCl₂, and 20 μ L of 5 mmol/L p-nitrophenyl phosphate (PNPP) were added to the supernatant. The mixture was left to react at 37°C for 30 minutes, and 50 μ L of 1 N NaOH was added to stop the reaction. Using PNPP as a standard, the absorbance was measured at 410 nm using a spectrophotometer. The ALP activity was expressed as the quantity of PNPP produced divided by the reaction time and the protein synthesis quantity, as measured by the Bio-Rad Protein Assay kit (Bio-Rad Laboratories, San Jose, California).

Immunofluorescence staining. The differentiation of osteoblasts was evaluated based on immunofluorescence staining for the RUNX2 gene. After 21 days of incubation, irrigation with PBS three times and stabilization with 4% paraformaldehyde for ten minutes, the cells were incubated with primary antibodies to the RUNX2 (1:100; Abcam, Cambridge, United Kingdom) overnight at 4°C. The cells were then incubated with secondary Alexa Fluor 594 goat anti-rabbit and mouse antibody (Invitrogen, Carlsbad, California) for one hour at room temperature. They were mounted with 4',6-diamino-2-phenylindole (DAPI) for ten minutes and then washed with PBS. We confirmed the differentiation of osteoblasts with colocalization by expression of DAPI and RUNX2 under high-powered magnification via confocal microscopy (Olympus, Tokyo, Japan).

Statistical analysis. We compared the mean cell proliferation assay and ALP activity of the cells on the two surfaces using a one-way analysis of variance (ANOVA) test. Statistical analysis was performed using SPSS 18.0 software (IBM, Armonk, New York, USA). Significance was defined as a p-value of less than 0.05.

Results

Scanning electron microscopy was used to study the morphology of the cells after six hours of *in vitro* incubation. The TPS (Fig. 2a) and DMF (Fig. 2b) surfaces were extensively covered with lamellipodia from the osteoblasts. Additionally, thin cytoplasmic projections (filopodia) extended into the interior of the pores. Osteoblasts on the surfaces of TPS and DMF covered more extensively, comparing machined Ti6Al4V (Fig. 2c) surfaces.

Adhesion of the cells was similar in the TPS and DMF groups, as reflected in the expression and distribution of the RUNX2 gene (Fig. 3) and actin filament (Fig. 4). However, expression of RUNX2 gene and distribution of actin filament were showing better than machined Ti6Al4V (Figs 3c and 4c).

The TPS and DMF groups were statistically different compared with the machined Ti6Al4V group on 72 hours incubation ($p = 0.017$ and 0.016 , respectively) in cell proliferation assay of the osteoblasts. There was no statistically significant difference between the TPS and DMF groups ($p = 0.367$) (Fig. 5).

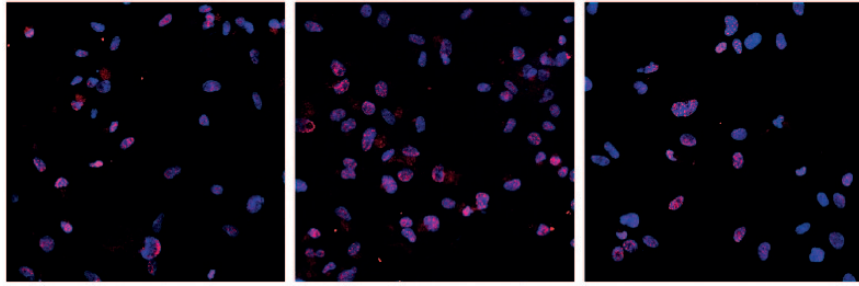


Fig. 3

Confocal microscopy images showing the expression and distribution of the RUNX2 gene in (a) titanium plasma spray (TPS)-coated specimens (x 200), (b) direct metal fabrication (DMF)-coated specimens (x 200), and machined (x 200) specimens. Note the similar staining intensity of RUNX2 (red dots) in the nuclei for TPS and DMF groups.

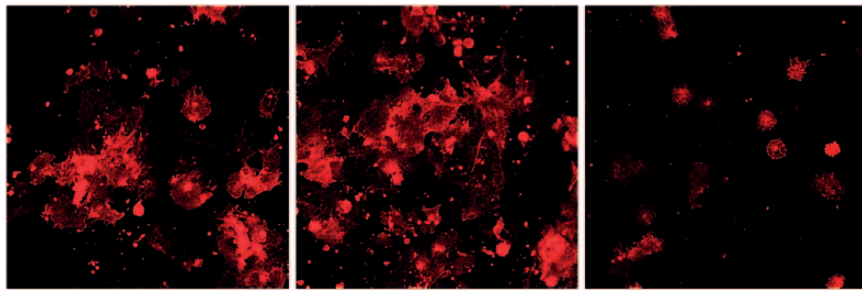


Fig. 4

Confocal microscopy images showing the expression and distribution of actin filaments in (a) titanium plasma spray (TPS)-coated specimens (x 100), (b) direct metal fabrication (DMF)-coated specimens (x 100), and machined Ti6Al4V (x 100) specimens. Note the similar staining intensity of actin filaments (red lines) around the cytoplasm for the TPS and DMF groups.

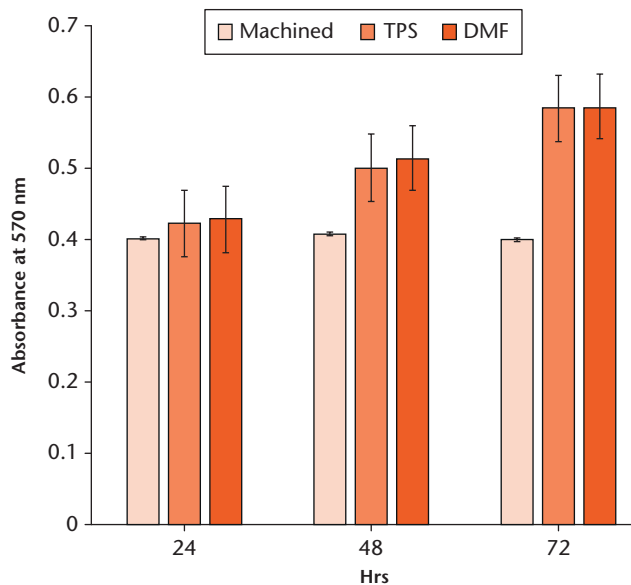


Fig. 5

Results (mean + SD) of osteoblast cell proliferation assays at 24, 48 and 72 hours for titanium plasma spray (TPS)-coated specimens, direct metal fabrication (DMF)-coated specimens and machined specimens. The cell proliferation assay difference was not statistically significant between the TPS and DMF groups ($p = 0.367$).

The ALP of the TPS and DMF groups were not statistically significantly different comparing with the machined group ($p = 0.021$ and 0.034 , respectively) and there

were insignificant differences between DMF and TPS groups ($p = 0.416$) (Fig. 6).

Discussion

The morphology, proliferation, and ability to differentiate of osteoblasts were used to investigate the biological response of TPS and DMF coatings of Ti alloys. The study had limitations. First, we assessed only *in vitro* effects on cell morphology, proliferation and differentiation. Further studies are needed to compare these coatings, which have not yet been studied *in vivo*. Secondly, a DNA study was not performed. Such a study could enhance the impact of these findings by also assessing the levels of type I collagen and osteocalcin.

The mean porosity ($65\% \pm 5\%$) of the DMF specimens was within the range of porosity for human cancellous bone (50% to 90%), but that of the TPS specimens ($40\% \pm 5\%$) was not. Also, despite the inferior mechanical and physical characteristics of the coating structure due to the approximately 1.6-fold higher porosity, the DMF specimens had comparable, if not better, mechanical and physical properties to those of the current commercial TPS specimens, suggesting that DMF creates a more favourable biomimetic porous structure than TPS. Therefore, DMF should be regarded as a more appropriate surface coating for cementless arthroplasty than the existing TPS technology. As DMF can control porosity, it

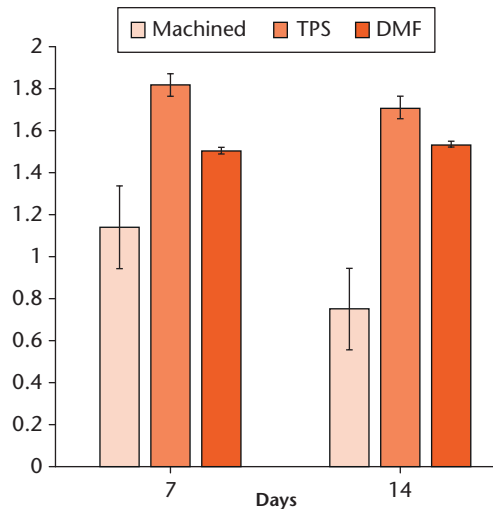


Fig. 6

Results (mean + SD) of alkaline phosphatase (ALP) activities of osteoblasts at seven and 14 days for titanium plasma spray (TPS)-coated specimens, direct metal fabrication (DMF)-coated specimens and machined specimens. The differences in the ALP activities between the TPS and DMF groups were not statistically significant ($p = 0.416$).

could be used to create a patient-specific porous structure for cementless arthroplasty.^{14,16}

The cell morphology and proliferation assay indicated that all the surfaces were cytocompatible. The cell proliferation in the DMF and TPS groups was not statistically different. Osteoblasts on the surface of DMF specimens spread and formed lamellipodia, as they also did on the TPS specimens, indicating that the two surfaces had similar cytocompatibility. Expressions of RUNX2 gene and actin filament, and ALP activity are indicators of osteogenic differentiation, bone formation and matrix mineralization.¹⁷⁻¹⁹ The DMF and TPS groups were not significantly different for these expressions indicating that the two surfaces had similar effects on the differentiation, bone formation and matrix mineralization of human osteoblasts.

We found that the coating produced by DMF with metal 3D printing was similar to that produced with TPS, which is the most commonly used coating for bone ingrowth. We introduced 3D printing deposition with DMF with the hypothesis that the combination could improve the morphology, proliferation, and ability of osteoblasts to differentiate *in vitro* to coated Ti6Al4V compared with the conventional plasma spray method. The DMF and TPS groups displayed similar surface characteristics in their ability to osseointegrate and their biomechanical quality. Hence, the method of using 3D printing with DMF provided an acceptable surface structure and a viable biological surface. Moreover, this method is automatable and less complex than plasma spraying. Thus, DMF with 3D printing is a novel and efficient method that could be used to create and process prostheses. Using this technique in conjunction with laser welding could enable the manufacture of components with various configurations.

References

- Khanuja HS, Vakili JJ, Goddard MS, Mont MA. Cementless femoral fixation in total hip arthroplasty. *J Bone Joint Surg [Am]* 2011;93-A:500-509.
- Abdulkarim A, Ellanti P, Motterlini N, Fahey T, O'Byrne JM. Cemented versus uncemented fixation in total hip replacement: a systematic review and meta-analysis of randomized controlled trials. *Orthop Rev (Pavia)* 2013;5:e8.
- Harvey EJ, Bobyn JD, Tanzer M, et al. Effect of flexibility of the femoral stem on bone-remodeling and fixation of the stem in a canine total hip arthroplasty model without cement. *J Bone Joint Surg [Am]* 1999;81-A:93-107.
- Yamada H, Yoshihara Y, Henmi O, et al. Cementless total hip replacement: past, present, and future. *J Orthop Sci* 2009;14:228-241.
- Yamauchi R, Itabashi T, Wada K, et al. Photofunctionalised Ti6Al4V implants enhance early phase osseointegration. *Bone Joint Res* 2017;6:331-336.
- Itabashi T, Narita K, Ono A, et al. Bactericidal and antimicrobial effects of pure titanium and titanium alloy treated with short-term, low-energy UV irradiation. *Bone Joint Res* 2017;6:108-112.
- Pijls BG, Sanders IMJG, Kuijper EJ, Nelissen RGHH. Non-contact electromagnetic induction heating for eradicating bacteria and yeasts on biomaterials and possible relevance to orthopaedic implant infections: *In vitro* findings. *Bone Joint Res* 2017;6:323-330.
- Matassi F, Botti A, Sirleo L, Carulli C, Innocenti M. Porous metal for orthopedics implants. *Clin Cases Miner Bone Metab* 2013;10:111-115.
- Engh CA, Hooten JP Jr, Zettl-Schaffer KF, et al. Porous-coated total hip replacement. *Clin Orthop Relat Res* 1994;298:89-96.
- Engh CA, Massin P. Cementless total hip replacement using the AML stem. 0-10 years results using a survivorship analysis. *Nihon Seikeigeka Gakkai Zasshi* 1989;63:653-666.
- Chen CJ, Xenos JS, McAuley JP, Young A, Engh CA Sr. Second-generation porous-coated cementless total hip arthroplasties have high survival. *Clin Orthop Relat Res* 2006;451:121-127.
- Lombardi AV Jr, Berend KR, Mallory TH, Skeels MD, Adams JB. Survivorship of 2000 tapered titanium porous plasma-sprayed femoral components. *Clin Orthop Relat Res* 2009;467:146-154.
- Karageorgiou V, Kaplan D. Porosity of 3D biomaterial scaffolds and osteogenesis. *Biomaterials* 2005;26:5474-5491.
- Shin T, Park S-J, Kang KS, et al. A laser-aided direct metal tooling technology for artificial joint surface coating. *Int J Precis Eng Manuf* 2017;18:233-238.
- Ryan G, Pandit A, Apatsidis DP. Fabrication methods of porous metals for use in orthopaedic applications. *Biomaterials* 2006;27:2651-2670.
- Balla VK, Banerjee S, Bose S, Bandyopadhyay A. Direct laser processing of a tantalum coating on titanium for bone replacement structures. *Acta Biomater* 2010;6:2329-2334.
- Le Guéhennec L, Soueidan A, Layrolle P, Amouriq Y. Surface treatments of titanium dental implants for rapid osseointegration. *Dent Mater* 2007;23:844-854.
- Zhao W, Zhang S, Wang B, et al. Runx2 and microRNA regulation in bone and cartilage diseases. *Ann N Y Acad Sci* 2016;1383:80-87.
- Shin JW, Swift J, Ivanovska I, et al. Mechanobiology of bone marrow stem cells: from myosin-II forces to compliance of matrix and nucleus in cell forms and fates. *Differentiation* 2013;86:77-86.

Funding Statement

- None declared

Acknowledgements

- T. Shin and D. Lim are co-first authors.
- This work was supported by the Advanced Technology Center (project number: 10048394) from the Korea Evaluation Institute of Industrial Technology (KITECH). The Catholic master cells supplied by the Catholic Institute of Cell Therapy (CIC, Seoul, South Korea) were derived from human bone marrow donated by healthy donors after informed consent.

Author Contributions

- T. Shin: Conducting the experiment, Analysing the results, Drafting the manuscript.
- D. Lim: Analysing the results, Drafting the manuscript.
- Y.S. Kim: Designing the experiment, Analysing the results.
- S.C. Kim: Conducting the experiment, Statistical analysis.
- W.L. Jo: Editing the manuscript, Statistical analysis.
- Y.W. Lim: Designing the experiment, Analysing the results, Editing the manuscript.

Conflict of Interest Statement

- None declared

© 2018 Author(s) et al. This is an open-access article distributed under the terms of the Creative Commons Attribution licence (CC-BY-NC), which permits unrestricted use, distribution, and reproduction in any medium, but not for commercial gain, provided the original author and source are credited.